Journal Name

ARTICLE

Alumina Grafted SBA-15 Sustainable Bifunctional Catalysts for Direct Cross-Coupling of Benzylic Alcohols to Diarylmethanes

Chandran Rajendran[a], Govindaswamy Satishkumar[a]*, Charlotte Lang[b] and Eric M. Gaigneaux[b]

Received 00th January 20xx,
Accepted 00th January 20xx

DOI: 10.1039/x0xx00000x

www.rsc.org/

AlSBA-15 catalysts possessing Brønsted acid and Lewis acid-base bifunctionalities catalyze the direct arylation of benzyl alcohol to diarylmethanes with 85% product yield through C-O bond activation. 2 and 4wt%AlSBA-15 catalysts have been synthesised by adopting a simple and efficient post-synthetic metal implantation route. The synthesised catalysts were characterized using XRD, N_2 adsorption and desorption, ^{27}Al MAS NMR, XPS, HR-TEM, NH_3 and CO_2-temperature-programmed desorption (TPD) and pyridine-Transmission-FTIR spectroscopy techniques to confirm the existence of Brønsted acid and Lewis acid-base bifunctionalities. Through various control experiments, it is verified that Brønsted acid sites activate the benzyl alcohol and Lewis base sites interact with Phenylboronic acid concurrently to accomplish the coupling reaction. In the recyclability study, 4wt%AlSBA-15 preserves its activity and stability up to 5 cycles. 4wt%AlSBA-15 catalyst unlike the homogenous catalysts does not require additives, long reaction time and expensive metals.

Introduction

Diarylmethanes are common structural constituents in biologically active drugs[1,2] and supramolecules[3,4]. Usage of conventional acids/Lewis acids as catalysts to synthesise diarylmethane have been replaced by transition metal catalysts in the last few decades. However, largely, highly reactive electrophiles such as benzyl halides and their equivalents have been used as coupling partner despite their environmental footprint. Among the various available environmental benign electrophiles, the easily available benzyl alcohol and its derivatives are preferred in the direct arylation since it is a step- and atom-economic reaction[5-8]. On the other hand, there are hurdles that have to be dealt with alcohols like high C-O bond dissociation energy, the poor leaving tendency of its -OH group, and the necessary protection of this -OH group while activating the C-O bond. Therefore, highly active alcohols such as allylic[9-12], allenylic alcohols[13] and propargylic alcohols[14] have been widely applied in cross-coupling reactions. Z.-J. Shi et al. first reported the nickel catalyzed direct cross-coupling of benzyl alcohols as coupling partner to synthesise diarylmethane using excess Grignard reagent (Scheme 1a)[15]. Later, Shi's group has reported $Pd(PPh_3)_4$-catalyzed synthesis of diarylmethane using benzyl alcohol through Suzuki–Miyaura coupling in the absence of any additives (Scheme 1b)[16]. Recently, S.M. Samec et al. have reported the nickel catalyzed Suzuki coupling reaction involving primary and secondary naphthyl and quinolyl alcohols and boronic acids to produce diarylmethane (Scheme 1c)[17]. Nevertheless, in the above examples, the high reactivity of Grignard reagent as a partner, the poor functional group tolerance, the use of expensive palladium catalysts, the need of a base and extended reaction time, are shortcoming which limits their potential applications. Interestingly, Shi et al. have proposed that Lewis acidity of the boronic acid derivatives and the Lewis basicity of benzyl alcohol is strong enough to activate each other to facilitate the desired cross-coupling through the formation of borates[16]. This concept stimulated us to examine for the same reaction mesoporous solid catalysts having immobilized bifunctionalities like Brønsted acid sites to activate the benzyl alcohol and Lewis basic sites to interact with Phenylboronic acid, and to accomplish the desired cross-coupling reaction.

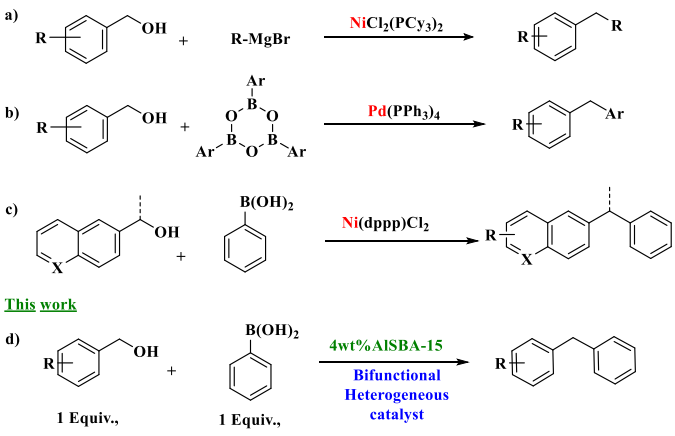

Scheme 1. Various approach for the synthesis of diarylmethane using benzyl alcohols and arylboronic acid.

a C. Rajendran and Dr. G. Satishkumar,
Advanced Materials and Catalysis Lab, Department of Chemistry,
School of Advanced Sciences, Vellore Institute of Technology, Vellore-632014,
Tamilnadu, India. Tel: +91-416-2202714.
E-mail: satishkumar.g@vit.ac.in; satishgsamy@gmail.com.
b Prof. Eric M. Gaigneaux and Dr. Charlotte Lang
Institute of Condensed Matter and Nanosciences, UCLouvain,
1348 Louvain-la-Neuve, Belgium.
† Footnotes relating to the title and/or authors should appear here.
Electronic Supplementary Information (ESI) available: [details of any supplementary information available should be included here]. See DOI: 10.1039/x0xx00000x

In the past few decades owing to its easy separation and recovery, heterogeneous catalysis has been attracting much attention in pharmaceutical and fine chemical synthesis. The possibility of assembling multi-functionalities at the solid surface of heterogeneous catalysts significantly enhances its capacity to catalyze various organic reactions[18,19]. In particular, high surface area mesoporous supports could immobilize two or more functionalities in their channels at an appropriate distance, which is difficult or impossible to achieve in solution, thus catalyze multistep or consecutive reactions by cooperative effects. In recent years, considerable efforts have been made to develop mesoporous acid-base bifunctional catalysts with different strengths by introducing diverse acids like sulfonic acids[20], carboxylic acids[21], phosphotungstic acids[22], Al-doped silica frameworks[23] and bases like primary, secondary, tertiary amines[24-26], or alkaline earth metal oxides[27] into the mesoporous matrix. The widely adopted synthetic strategies to covalently introduce the functional groups into the mesoporous silica matrix are co-condensation or grafting routes. In case of grafting procedure often the basic amine sites are created by the hydrolysis of alkoxide bonds followed by condensation with the silanols in the mesoporous matrix. Grafting of second functionality in the same mesoporous silica matrix is highly challenging as the undesired mutual quenching of acid and base sites is possible[28]. Hence one way to avoid this quenching issue is that one of the reactive components is protected during the grafting procedure to avoid acid-base site interaction. Later, acid or base and thermal treatment can cleave the protecting group. However, the grafting method has several drawbacks like partial pore blocking, the stability of the silica matrix and the second functional group can be affected due to essential acid or base and thermal treatment, respectively. In the co-condensation method, the functional groups are introduced in the synthesis gel during the preparation of mesoporous material. Although this technique avoids the issues associated with the grafting procedure, complete removal of the template is highly challenging and causes serious problems to the attached functional groups. Hence, there is a need for developing an easy, efficient method to immobilise two or more functionalities in the mesoporous support. Interestingly, by varying the grafting aluminium weight % over the mesoporous silica support, it is possible to generate Brønsted acid and Lewis acid-base bifunctionalities through metal implantation method[29]. However, to the best of our knowledge, this type of bifunctional catalysts is less exploited for catalysis.

Herein, aluminium containing mesoporous bifunctional catalysts possessing Brønsted acid and Lewis acid-base functionalities have been synthesised by adopting a simple and efficient post-synthetic metal implantation route. The synthesised catalysts were used to catalyze the reaction between 2-naphthylmethanol and phenylboronic acid to construct the 2-benzyl naphthalene (Scheme 1d). 2 and 4 weight % of aluminium has been grafted over the mesoporous silica SBA-15 followed by calcination at high temperature. During the high-temperature thermal treatment part of the grafted aluminium ions get into the silica Framework thereby generating Brønsted acid sites. Whereas, the remaining aluminium ions form alumina clusters contain Lewis acid-base sites in the mesoporous channels of SBA-15. To our delight, the best catalyst 4wt%AlSBA-15 catalyzed the reaction between 2-naphthalenemethanol and phenylboronic acid with a yield of 85% to the coupled product. The synthesised catalysts have been thoroughly characterized using XRD, N_2 adsorption and desorption, HR-TEM, ^{27}Al MAS NMR, XPS, NH_3 and CO_2- temperature-programmed desorption (TPD) and pyridine-Transmission-FTIR spectroscopy techniques to understand the cooperative effect of the functionalities (Brønsted acid and Lewis base) to catalyze the reaction. Based on this understanding a plausible mechanism has been proposed for the derived coupled product involving the Brønsted acid and Lewis base sites.

Experimental

Synthesis of 2, 4wt%AlSBA-15 and γ-Al_2O_3

Mesoporous silica SBA-15 was synthesised through a hydrothermal technique using P_{123} triblock copolymer structure directing agent as reported in the literature[30]. The grafting of 2 and 4wt% alumina over the SBA-15 was done by following the procedure proposed in the literature[31]. In brief, 1 ml of trimethylamine and 1 g SBA-15 were introduced to the solution containing 5.8 g of $Al(O\text{-}sec\text{-}Bu)_3$ (correspond to 4wt% Al) and anhydrous toluene (100 ml) at 85°C. The reaction mixture was stirred continuously for 6 h. The solid was separated by filtration, washed with toluene, and dried. The obtained dry solid was added to 30ml of ethanol and hydrolysed at 25°C for 24 h. Finally, the solid was washed with ethanol, filtered and then dried in air at 120°C. Finally, the acid part of the bifunctionality has been created by heating the dried sample at 550°C for 10h at a heating rate 1°C/min through metal implantation method[29]. γ-Al_2O_3 has been synthesised by following the above procedure without mesoporous silica support.

Synthesis of IE4wt%AlSBA-15M

AlSBA-15 having aluminium exclusively in the tetrahedral symmetry was synthesised by following the recipes given in the literature[32]. In brief, 1 g of silica SBA-15 in 50 mL of water containing 0.122g of sodium aluminate stirred at room temperature for 12 h. The solid material was then filtered, washed with distilled water, and dried at room temperature in air. Further, it is calcined at 550°C for 5h and the obtained material is designated as 4wt%AlSBA-15M (M-Modified). Subsequently, 4wt%AlSBA-15M sample was ion-exchanged using 1M ammonium nitrate solution refluxing at 100°C for 3h[33]. The obtained material was filtered and the above ion exchange procedure was repeated thrice and dried overnight at 100°C. Finally, to obtain IE4wt%AlSBA-15M (IE-Ion-exchanged) dried sample was calcined at 550°C for 5h.

Synthesis of CeO_2

0.5g of Cerium nitrate was dissolved in 30 ml water and 1M NaOH solution was added and stirred for 1h at room temperature. Then, the solid material was filtered, washed with distilled water, and dried at room temperature in air and calcined at 550°C for 1h.

Synthesis of CeO_2/IE4wt%AlSBA-15M

0.027g of $Ce(NO_3)_3.6H_2O$ (corresponding to 2wt%) was dissolved in 10 ml of distilled water and impregnated on 0.5g of IE4wt%AlSBA-15. This suspension was stirred overnight at 80°C until dried and the sample was calcined at 550°C for 1h.

Catalytic studies

The reaction was carried out by addition of 100mg AlSBA-15 catalyst to the mixture of 1 equiv. of 2-napthalenemethanol (0.3 mmol), 1 equiv. of phenylboronic acid (0.3 mmol), in 2-3ml of dichloroethane solvent. The reaction mixture was stirred at 80°C for 6 h in N_2 atmosphere. After cooling, the reaction mixture was stirred with 10ml of ethyl acetate and the catalyst was separated from the reaction mixture by filtration. The filtrate was further concentrated to remove the solvent and used for GC-MS analysis. For column chromatography, 1.5 g of silica gel (100-200 mesh) was added to the residue and purified by eluting with hexane to get the desired isolated product.

Results and discussion

The low-angle XRD pattern of 2 and 4wt%AlSBA-15 shown in Fig. S1† displayed a high intensity peak (100) beside two less intensive reflections corresponding to the hexagonal arrangement of the mesopores in SBA-15[30]. The amorphous wide-angle XRD pattern of 2 and 4wt%AlSBA-15 (Fig. S2†) corroborates the absence of bulk alumina crystals in the mesopores of SBA-15. The synthesised alumina displayed typical wide-angle XRD pattern corresponding to γ-Alumina[34] (JCPDS No. 29-0063). The physicochemical properties of the synthesised materials are summarized in Table 1. The surface area of 2 and 4wt%AlSBA-15 decreased to 798 and 743 m^2/g respectively from its parent SBA-15's surface area of 902 m^2/g. The micropore surface area decreases from 109 to 79 m^2/g upon 2wt% alumina grafting. In the case of 4wt%AlSBA-15, micropore surface area remains essentially unaltered indicating that subsequent grafting of aluminium ion proceeds into the mesopores of the support SBA-15. The synthesised γ-Alumina also possesses a good surface area of 241 m^2/g. Interestingly, alike parent SBA-15, 2 and 4wt%AlSBA-15 exhibit typical type IV isotherm characteristic of ordered mesopores endorsing the successful grafting of alumina without blocking the mesopores of the SBA-15 (Fig. S3†). Fig. S4† (A and B) shows the HR-TEM images of 2 and 4wt%AlSBA-15 catalysts recorded at different magnifications with corresponding EDAX data. TEM images confirm the successful grafting of 2 and 4wt%Al over the SBA-15 support by preserving the mesoscopic channels. Fig. S5† displays SEM-EDAX mapping of 2 and 4wt%AlSBA-15. The obtained results suggest that the weight % of Al in both the materials are close to the theoretical values and the elemental mapping confirms the uniform distribution of Al all over the SBA-15 particles.

In the interest of describing the state of distributed Al in the mesopores of SBA-15 the synthesised materials was further characterized using ^{27}Al MAS NMR, and XPS techniques. ^{27}Al MAS NMR spectra of 2wt%AlSBA-15 shown in Fig. 1 displayed two resonance signals centered at ca. 60 and 10 ppm endorsing the presence of tetrahedral (framework) and octahedral (extra framework) Aluminium species like in γ-Alumina, respectively[35,36]. High thermal treatment implemented during the grafting process implants part of the grafted Al into silica framework which can generate the Brønsted acid site and the remaining Al in the extraframework exists as alumina clusters having Lewis acid-base property (Scheme 2). It is interesting to note that 4wt%AlSBA-15 exhibited a major peak at ca. 10 ppm along with small peaks at ca. 60

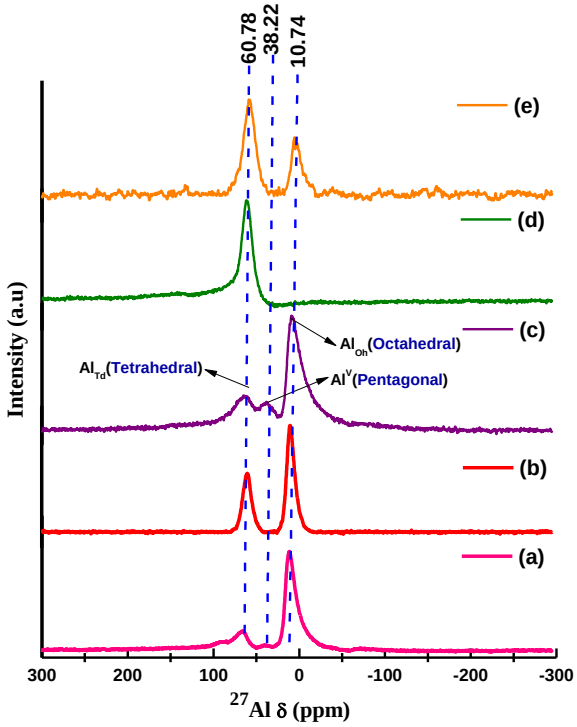

Fig. 1. ^{27}Al MAS NMR spectra for Al samples: (a) γ-Al_2O_3, (b) 2wt%AlSBA-15 (c) 4wt%AlSBA-15 (d) 4wt%AlSBA-15M (e) IE4wt%AlSBA-15.

Table 1 Physicochemical Characterization of Synthesised Catalysts

Entry	Material	Al weight (%)[a]	Al weight (%)[b]	Total Surface area (m^2/g)	Meso. area (m^2/g)	Micro. area (m^2/g)	Pore volume (cm^3/g)	Pore Diameter (nm)
1	SBA-15	-	-	902	793	109	1.69	7
2	2wt%AlSBA-15	2	2.2	798	719	79	1.42	4
3	4wt%AlSBA-15	4	3.9	743	681	62	1.23	4
4	γ-Al_2O_3			241	-	-	-	-

[a]Nominal weight percentage. [b]Weight percentage obtained from SEM-EDAX.

and 38 ppm which are attributed to aluminium in octahedral, tetrahedral and pentahedral environment respectively[36,37]. It was claimed that amorphous silica-alumina materials generate Brønsted acid sites through pseudo-bridging silanol groups, having arisen due to the interaction of terminal silanols with neighbouring coordinatively unsaturated aluminium atoms (pentahedral), which expedites the activation of the hydroxyl group in alcohols as leaving group[38]. Further, the intense extraframework aluminium peak in 4wt%AlSBA-15 indicates that it has more alumina clusters in the mesopores of SBA-15 compared to 2wt%AlSBA-15 in which part of the grafted aluminium clogged in the micropores (Table 1). XPS spectra of 4wt%AlSBA-15 in the binding energy region of Si2p, Al2p, exhibit multiple chemical shifts owing to silica-alumina interface (Fig. 2). Successful grafting of alumina with the silanols of mesoporous support has been confirmed through the appearance of Si2p components at 103.2 and 102.0 eV corresponding to Si-O-Si and Al-O-Si linkages. Likewise, the existence of alumina clusters in the mesopores of 4wt%AlSBA-15 is verified through Al2p binding energy peaks at 73.1 and 74.2 eV which correspond to Al-O-Si and Al-O-Al linkage[39].

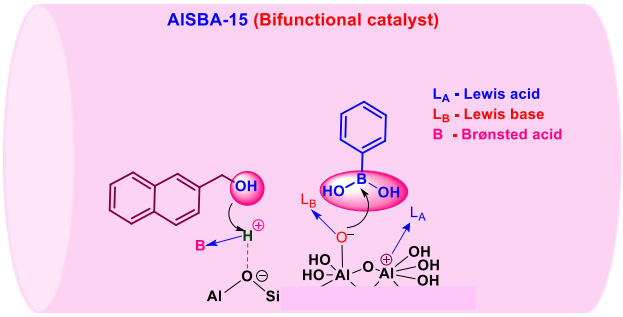

Scheme 2. Graphical illustration of the synthesised bifunctional 4wt%AlSBA-15 catalyst.

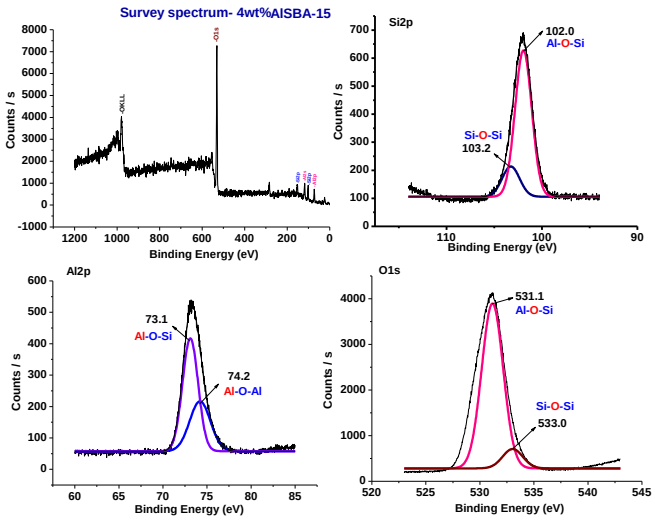

Fig. 2. XPS Spectra of catalyst 4wt%AlSBA-15

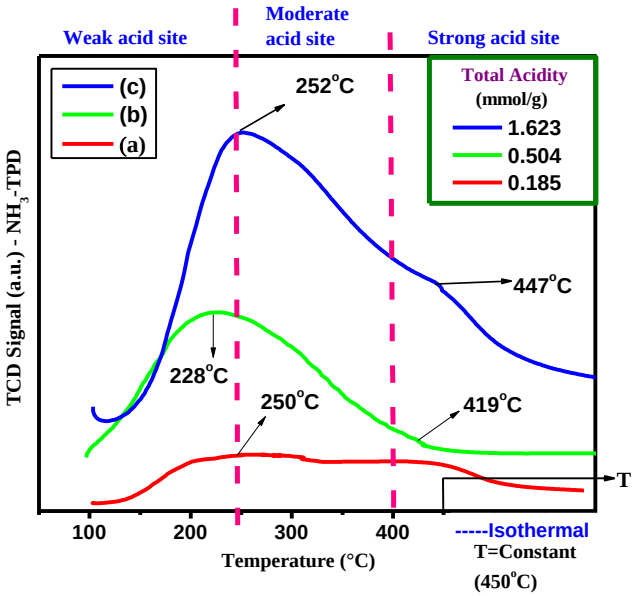

Fig. 3. NH_3-TPD Analysis for (a) γ-Al_2O_3, (b) 2wt%AlSBA-15 and (c) 4wt%AlSBA-15.

Ammonia and pyridine-Transmission-FTIR studies on acid sites of synthesised catalysts

Furthermore, in the catalysis perspective, it is essential to estimate the acid sites available in the synthesised catalysts. Therefore, synthesised catalysts γ- Alumina, 2 and 4wt%AlSBA-15 have been investigated using ammonia-TPD (Fig. 3) and the total acidity is recorded. Generally in NH_3-TPD studies, ammonia desorb from weak acid sites at below 200 °C; on the other hand, moderate and strong acid sites desorb the ammonia molecule between 250 to 350°C and 350 to 450°C, respectively[36,40]. It can be seen that there is a clear increase in the total acidity count from γ- Alumina to 4wt%AlSBA-15 (Fig. 3, inset). The total acidity count for γ- Alumina (0.185 mmol/g) is solely arisen from its moderate acid sites. Moderate and strong acid sites exist in both 2 and 4wt%AlSBA-15 catalysts as they have displayed two ammonia desorption peaks at ca. 250 and 450°C. It is interesting to note that substantial increase in the total acidity count was observed for 4wt%AlSBA-15 (1.623 mmol/g) compared to 2wt%AlSBA-15 (0.504 mmol/g) (Fig. 3, inset). Higher Aluminium loading and additional Brønsted acidity emanating from pseudo-bridging silanol groups have contributed to the increased acidity of 4wt%AlSBA-15 catalyst. Although NH_3-TPD technique has been broadly used to quantify the total acid sites, owing to its high reactivity with catalyst surface via hydrogen bonding it does not provide information on the Brønsted /Lewis distribution of the probed sites[40-42]. Thus, it has been decided to examine the synthesised catalysts γ- Alumina, 2 and 4wt%AlSBA-15 by pyridine-Transmission-FTIR spectroscopy technique. Fig. 4 illustrates the IR spectra of adsorbed pyridine at room temperature, 100 and 200°C on γ- Alumina, 2 and 4wt%AlSBA-15. Based on the adsorption coefficients, in situ transmission FTIR spectroscopy can be applied to quantify acid sites present in the catalyst [43-46]. The reported molar

extinction coefficients εL = 1.44 cm. µmol^{-1}and εB = 0.59 cm. µmol^{-1} (B = Brønsted acid and L = Lewis acid peaks.) were used for the estimation of acid sites present in the synthesised catalysts[47]. The spectra recorded at room temperature for all the three catalysts displayed peaks at 1623, 1493 and 1454 cm^{-1} corresponding to pyridine coordinating to Lewis acid sites. In case of 2 and 4wt%AlSBA-15, the peak at 1549 cm^{-1} and a shoulder at 1638 cm^{-1} are assigned to the pyridinium ions chemisorbed on the strong Brønsted acid sites[45]. As anticipated, peak corresponding to the Brønsted acid sites are completly missing for γ- Alumina (Fig. 4A) which complements the results obtained from ammonia-TPD (Fig. 3). Interestingly, for 2 and 4wt%AlSBA-15 catalysts after evacuation at 100°C, except the peaks at 1440 and 1590 cm^{-1} corresponding to weakly coordinated pyridine on Si-OH groups present in the mesoporous support SBA-15, all the other peaks remain present and even after evacuation at 200°C (Fig. 4B,C). This observation clearly suggests the availability of strong Lewis and Brønsted acid sites in 2 and 4wt%AlSBA-15 catalysts. The quantification of Lewis and Brønsted acid sites was done based on this Pyridine-Transmission-FTIR study (Fig. 4). IR spectra recorded after desorption at 100°C were used for the calculation of the distribution between Brønsted and Lewis acid sites and acidity calculation details are given in the supporting information page S4. Percentages of Lewis (65, 52%) and Brønsted acid sites (35, 49%) are available in the 2 and 4wt%AlSBA-15 catalysts, respectively. 4wt%AlSBA-15 comprises 2.5 fold higher Brønsted acid sites compared to 2wt%AlSBA-15 with almost equal distribution of Brønsted and Lewis acid sites. The total acidity count for all the catalysts derived from pyridine-Transmission-FTIR analysis is lesser than ammonia-TPD acidity data. This might be understood on the basis of the fact that unlike ammonia the bulkier aromatic pyridine can probe only accessible surface acid sites available in the catalyst. Hence, it was decided to use the acidity data obtained at 100°C from pyridine-Transmission-FTIR studies for Turn over number (TON) calculations of 2 and 4wt%AlSBA-15 catalysts.

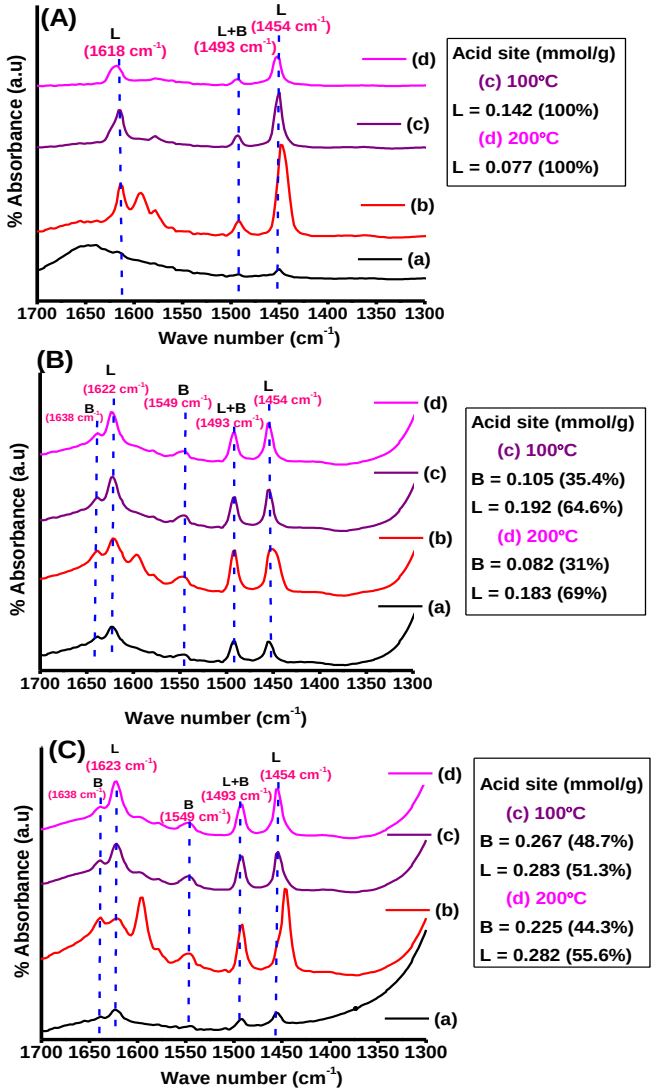

Fig. 4. Pyridine-Transmission-FTIR studies of synthesised catalysts (A) γ-Al_2O_3.; (B) 2wt%AlSBA-15; (C) 4wt%AlSBA-15. (a) Degassed at 250°C, (b) After pyridine adsorption, (c) After pyridine desorption 100°C, (d) After pyridine desorption 200°C: The extinction coefficients were used[47] εL = 1.44 cm. µmol^{-1} and εB = 0.59 cm. µmol^{-1} (B = Brønsted acid and L = Lewis acid peaks.)

Catalytic Activity

In an initial attempt, experiments were conducted to screen the best catalyst towards the cross-coupling between 2-naphthylmethanol and phenylboronic acid (Table 2. Entries 1-3). Among the catalysts, at the given conditions 4wt%AlSBA-15 proved to be more efficient compared to 2wt%AlSBA-15 and γ-Al_2O_3 and yielded after 24h 90% of the desired coupled product with a TON of 10. γ-Al_2O_3 which does not contain Brønsted acid sites exhibited poor catalytic performance whereas 2wt%AlSBA-15 demonstrated an intermediate catalytic activity with 60% yield to the coupled product. These results indicate the prerequisite of Brønsted acid sites in the catalyst to catalyze the above reaction. Subsequent optimization studies like time, temperature and solvent were carried out over the best catalyst, namely 4wt%AlSBA-15. The influence of time on the product yield was investigated and it was found that within 6 hours 85% of the product has been formed affording TON of 9.47 (Table 2, entries 6,7). From the temperature optimization studies, it is clear that temperature plays a critical role in the reaction. It was found that an increase in temperature from 60 to 70°C does not improve the yield (Table 2, entries 8, 9). However, rising the temperature to 80°C brought a better yield (Table 2, entry 7). It was observed that at 60°C reactants 2-naphthylmethanol and phenylboronic acid have completely converted and the desired product 2-benzyl naphthalene obtained as major product with 67% yield. At higher temperature (80°C) formation of side products found diminished and the coupled product yield has been improved to 85%. The formed byproducts have been identified through GC-MS analysis and details are given in the supporting information page S11. Among the various solvents examined like polar protic (Ethanol, H_2O), and polar aprotic (Acetonitrile, DMF, DMSO, THF, DCE), DCE appears to be the best solvent based on the product yield (Table 2, entries 10-15).

Table 2. Optimization of reaction conditions on 2-naphthalenemethanol with phenylboronic acid.

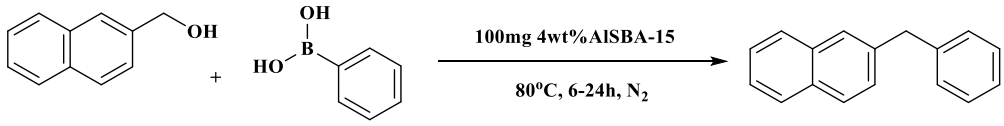

1, 0.3 mmol 2, 0.3 mmol 3a, 79% (90% GC yield)

Entry	Catalyst (100mg)	Solvent	Temp. (°C)	Time (h)	TON[(a)]	TOF[(b)] (h^{-1})	Yield (%)[(c)]
1	2wt%AlSBA-15	DCE	80	24	17.02	2.84	60
2	4wt%AlSBA-15	DCE	80	24	10.02	1.67	90 (79)[d]
3	γ-Al_2O_3	DCE	80	24	-	-	3
4	SBA-15	DCE	80	24	-	-	ND
5[e]	-	DCE	80	24	-	-	ND
6	4wt%AlSBA-15	DCE	80	12	9.69	1.62	87 (77)[d]
7	**4wt%AlSBA-15**	**DCE**	**80**	**6**	**9.47**	**1.57**	**85 (75)[d]**
8	4wt%AlSBA-15	DCE	60	6	7.46	1.24	67
9	4wt%AlSBA-15	DCE	70	6	7.79	1.29	70
10	4wt%AlSBA-15	Ethanol	80	6	-	-	ND
11	4wt%AlSBA-15	H_2O	80	6	-	-	ND
12	4wt%AlSBA-15	ACN	80	6	6.68	1.11	60
13	4wt%AlSBA-15	THF	80	6	6.68	1.11	60
14	4wt%AlSBA-15	DMF	80	6	-	-	ND
15	4wt%AlSBA-15	DMSO	80	6	-	-	ND
16	4wt%AlSBA-15M	DCE	80	6	-	-	ND
17	IE4wt%AlSBA-15M	DCE	80	6	-	-	35 (20)[d]
18	CeO_2/IE4wt%AlSBA-15M	DCE	80	6	-	-	60 (35)[d]

Reaction conditions: 1 (0.3 mmol), 2 (0.3 mmol) and catalyst (100mg) in solvent (2 mL) was stirred at 80°C for 6h and 24h under N_2 atmosphere; (a) Calculated by dividing the moles of product formed at 6h (21600 sec) by the moles of Brønsted acid sites present in the catalyst; (b) Calculated dividing TON by time; (c) Yield monitored by GC (n-Decane as internal standard); (d) Isolated yield; (e) Without catalyst; ND- Not Detected.

Role of Brønsted acid and Lewis base sites in the diarylmethane construction reaction

Despite the remarkable catalytic activity of 4wt%AlSBA-15 towards arylation of 2-naphthylmethanol, ambiguity still remains on the role of each active sites as the catalyst possesses both Brønsted and Lewis acid-base functionalities. Hence, further investigations are required to gain insight on the role of each functionality to produce the desired coupled product. To identify the involvement of Brønsted acid sites, the reaction was carried out using 2-pyridinemethanol as one of the reactants instead of 2-naphthylmethanol and in the other trial, 0.5 ml of pyridine was used in the reaction mixture under the same reaction conditions. In both the experiments 4wt%AlSBA-15 did not afford the desired product. Owing to the high basicity of 2-pyridinemethanol and pyridine molecules they likely preferentially adsorbed over the Brønsted acid sites of the 4wt%AlSBA-15 thus preventing the studied reaction to proceed. Earlier, it was noticed that γ-Al_2O_3 catalyst which does not have the Brønsted acid sites could not catalyze the coupling reaction. Hence, this observation reinforces the involvement of Brønsted acid site in the above reaction. To further confirm the participation of Lewis acid-base sites in the arylation of 2-naphthylmethanol it is decided to vary the composition of tetrahedral and octahedral aluminium in the 4wt%AlSBA-15 which in turn varies the Brønsted and Lewis acid-base sites and which consequently, would affect the coupled product yield. We synthesised 4wt%AlSBA-15M (M-modified) containing aluminium exclusively in the tetrahedral symmetry through post grafting technique using an aqueous solution of sodium aluminate[32] (Fig. 1d). As expected, 4wt%AlSBA-15M could not catalyze the reaction due to the presence of Na^+ ions which balance the negative charges associated with tetrahedral aluminium (Table 2, entry 16). Hence, 4wt%AlSBA-15M catalyst was ion exchanged with H^+ to replace the Na^+ ion and it is designated as IE4wt%AlSBA-15M. During the ion exchange process, the alkaline environment and high-temperature treatment generated extraframework aluminium species which is evidenced through the appearance of a resonance peak at ca 10 ppm in ^{27}Al MAS NMR shown in Fig. 1(e). Interestingly, contrarily to 4wt%AlSBA-15, IE4wt%AlSBA-15M possesses more aluminium in tetrahedral symmetry suggesting the presence of more Brønsted acid sites than Lewis acid-base sites. IE4wt%AlSBA-15M

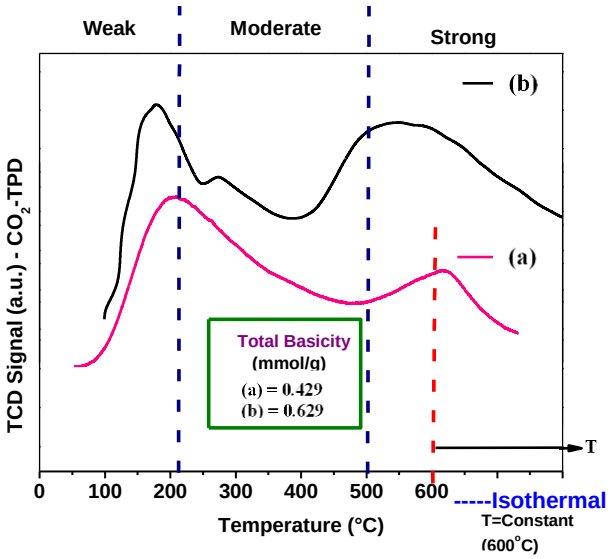

Fig. 5 CO_2-TPD Analysis of (a) 4wt%AlSBA-15; (b) CeO_2/IE4wt%AlSBA-15M

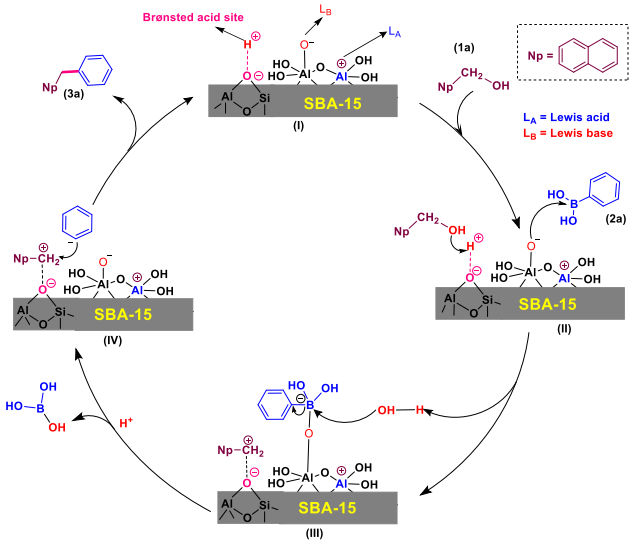

Scheme 3. Plausible mechanism of diarylmethane formation via benzylic C-O Bond Activation.

catalyzes the coupling reaction with 35% product yield (Table 2, entry 17). The insignificant existence of extraframework aluminium in IE4wt%AlSBA-15M thus severely affected the product yield. This observation strongly supports the significant role of alumina clusters in 4wt%AlSBA-15 which bring Lewis acid-base sites required in the studied reaction. It is anticipated that Lewis base sites in the alumina clusters of 4wt%AlSBA-15 alone can activate the phenylboronic acid through acid-base interaction. Therefore it was planned to impregnate well-known Lewis base cerium oxide (2wt%) into the mesopores of IE4wt%AlSBA-15M and the obtained sample was examined for the chosen coupling reaction. The wide-angle XRD pattern of CeO_2/IE4wt%AlSBA-15M catalyst displayed cerium oxide peaks which are in good agreement with the earlier report[48] (Fig. S6†).The surface basic properties of CeO_2/IE4wt%AlSBA-15M and 4wt%AlSBA-15 were studied through CO_2-TPD investigation as shown in the Fig. 5. Both the catalysts displayed desorption peak at ca below 200 °C and above 500 °C revealing the existence of weak and strong basic sites[49]. To our delight, the presence of cerium oxide in CeO_2/IE4wt%AlSBA-15M enhanced the product yield to 60% at the same reaction conditions (Table 2, entry 18). This observation validates the involvement of Lewis base sites in the activation of phenylboronic acid to accomplish the coupling reaction. Although CeO_2/IE4wt%AlSBA-15M has more basic sites (0.629mmol/g) than 4wt%AlSBA-15 (0.429mmol/g), the high dispersion of alumina clusters in 4wt%AlSBA-15 increases the accessibility of reactant molecules to produce a higher product yield. Therefore, based on the various characterization results and experiments attempted it is concluded that the bifunctionality, i.e. simultaneous presence of Brønsted acid and Lewis base sites, of 4wt%AlSBA-15 indeed participates in the reaction to yield the desired coupled product.

A plausible mechanism has thus been proposed involving the Brønsted acid and Lewis base sites in 4wt%AlSBA-15 (Scheme 3). Initially, 2-naphthylmethanol is protonated by the Brønsted acid sites; subsequently a water molecule is released. The formed benzylic carbocation was chemisorbed over the bridged oxygen anion of aluminosilicate framework. Concurrently, phenylboronic acid chemisorbed over the Lewis base site exposed by the alumina clusters to form boronate ion. The released water molecule protodeboronates the chemisorbed boronate ion to generate the transient aryl anion[50].

Table 3. Substrate variation of Boronic acids

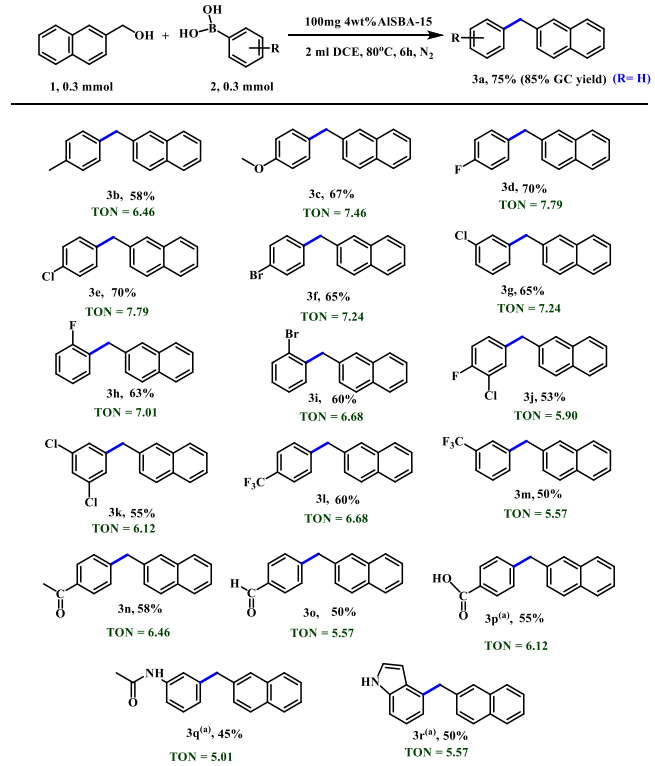

Reaction conditions: The solution of 1 (0.3 mmol), 2 (0.3 mmol) and catalyst (4wt%Al/SBA-15) (100mg) in DCE (2 mL) was stirred at 80°C for 6h under N_2 atmosphere. All are isolated yield product. (a) 130°C for 6h.

The formed transient aryl anion immediately reacts with nearby chemisorbed benzylic carbocation to give the desired coupled product. The released proton from the water molecule adsorbs over the bridged oxygen atom to regenerate the Brønsted acid site.

Under the optimized conditions, the tolerance of the catalyst to various functional groups was studied by varying functional groups in the phenylboronic acid and variety of arylmethanols (Table 3). Initially, variation of the boronic acid was explored. It was found that electron donating groups $–CH_3$ and $–OCH_3$ are compatible with the reaction conditions to give good yield. With the electron withdrawing substituents–4Cl,–4Br, –3Cl, –2F, –2Br, 4wt%AlSBA-15 demonstrated good yields. However, with the multi halo substituents (**3j, 3k**) depreciation in the yield was observed. Likewise, $3–CF_3$ and $4–CF_3$ induced decrease in the yield. Substituents like $–COCH_3$ and –CHO were tolerated to the optimized conditions. Furthermore, examples like 3p, 3q and 3r demanded harsher reaction conditions to achieve a better yield. Subsequently, variation of the benzylic alcohol was examined. Predictably, benzylic alcohol possessing electron donating and electron withdrawing substituents were compatible with the reaction conditions (**4a-h**, Table 4).

The privilege of using heterogeneous catalyst is acknowledged through its performance in recyclability study. Therefore, recyclability of 4wt%AlSBA-15 catalyst has been studied towards the cross-coupling between 2-naphthylmethanol and phenylboronic acid at the optimized conditions. After each run the catalyst was recovered by filtration and washed thoroughly with ethyl acetate solvent (10ml). Further, the catalyst was dried overnight at 100 °C and employed for the next run. The catalyst maintained its high activity and stability up to 5 cycles (Fig. 6).

Table 4. Substrate variation of Benzylic alcohols

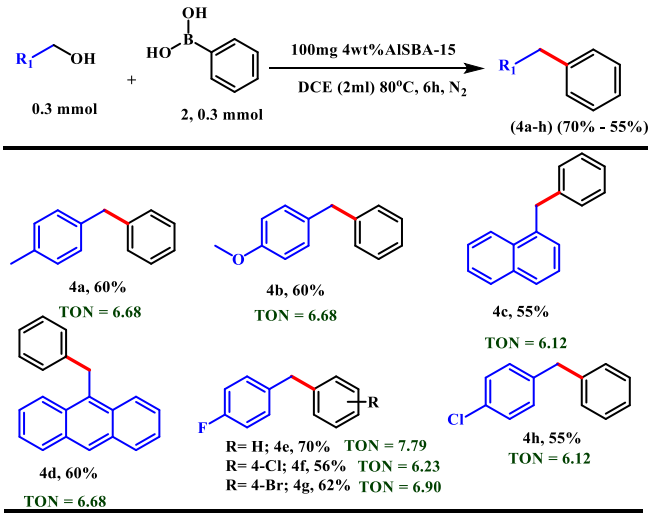

Reaction conditions: The solution of 1 (0.3 mmol), 2 (0.3 mmol) and catalyst(4wt%Al/SBA-15) (100mg) in DCE (2 mL) was stirred at 80°C for 6h under N_2 atmosphere. All are isolated yield product.

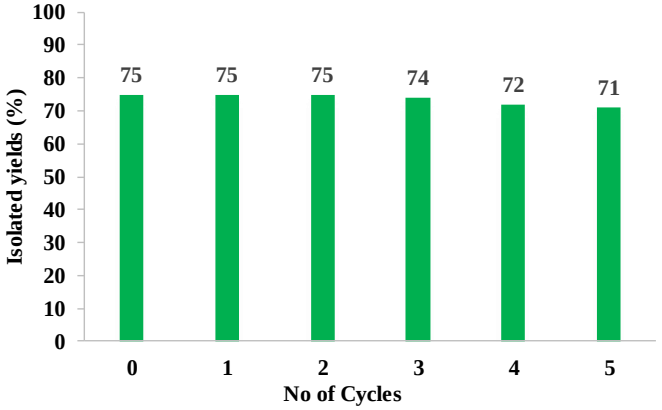

Fig. 6 Recyclability study of catalyst 4wt%AlSBA-15 in the arylation of 2-naphthylmethanol at the optimized conditions.

Spent catalyst after 5 cycles was characterized using wide-angle XRD and SEM-EDAX (Fig. S9† and S10†). The SEM-EDAX results confirm the presence of 3.73wt% of Al in the spent catalyst after 5 cycles. Further, amorphous XRD pattern of spent4wt%AlSBA-15 catalyst assures that the aluminium incorporated in the framework and grafted alumina clusters on the mesopores of the support SBA-15 are intact.

Conclusions

In this study, 4wt%AlSBA-15 conclusively proved as an efficient, stable and sustainable heterogeneous catalyst towards the construction of biarylmethane using 2-naphthylmethanol and phenylboronic acid through C-O bond activation. Bifunctionality, i.e. the simultaneous presence of Brønsted acid and Lewis acid-base sites, is easily introduced in the mesopores of SBA-15 by implementing simple and efficient post-synthetic metal implantation route.The high catalytic performance of 4wt%AlSBA-15 indicates the significance of heterogeneous catalysts having bifunctionality in activating the reactant molecules through cooperative effect. Detailed characterization and different control experiments revealed that Brønsted acid and Lewis base sites both played a critical role to deliver the desired coupled product by activating the 2-naphthylmethanol and Phenylboronic acid, respectively. Stability of the 4wt%AlSBA-15 catalyst is evidenced through its consistent performance in 5 consecutive cycles. Compared to homogeneous catalysts, 4wt%AlSBA-15 does not require additives, long reaction time and expensive metals. This study opens a new path to employ bifunctional heterogeneous catalyst in academic research and chemical industries for challenging organic transformations.

Conflicts of interest

"There are no conflicts to declare".

Acknowledgements

This study was financially supported by VIT transdisciplinary grant from VIT management. Authors thank SIF-IISC Bangalore for Solid state NMR and VIT-SIF for ^{1}H and ^{13}C NMR.

Notes and references:

1. A. Gangjee, R. Devraj, S. F. Queener, *J. Med. Chemistry,* 1997, **40**, 470-478.
2. A. V. Cheltsov, M. Aoyagi, A. Aleshin, E. C. W. Yu, T. Gilliland, D. Zhai, R. Abagyan, *J. Med. Chemistry,* 2010, **53**, 3899-3906.
3. M. M. Conn, J. Rebek, *Chem. rev.,* 1997, **97**, 1647-1668.
4. A. Jasat, J. C. Sherman, *Chem. rev.,* 1999, **99**, 931-968.
5. McLaughlin, M., *Org. Lett.,* 2005, ***7***, 4875-4878.
6. C. C. Kofink, P. Knochel, *Org. Lett.,* 2006, **8**, 4121-4124.
7. M. R. Harris, L. E. Hanna, M. A. Greene, C. E. Moore, E. R. Jarvo, *J. Am. Chem. Soc.,* 2013, ***135***, 3303-3306.
8. R. Kumar, E. V. Van der Eycken, *Chem. Soc. Rev.,* 2013, **42**, 1121-1146.
9. B. M. Trost, J. Quancard, *J. Am. Chem. Soc.,* 2006, **128**, 6314-6315.
10. Y.-X. Li, Q.-Q. Xuan, L. Liu, D. Wang, Y.-J. Chen, C.-J. Li, *J. Am. Chem. Soc.,* 2013, **135**, 12536-39.
11. J. Ye, J. Zhao, J. J. Xu, Y. Mao, Y. J. Zhang, *Chem. Commun.,* 2013, **49**, 9761-63.
12. H.-B. Wu, X.-T. Ma, S.-K. Tian, *Chem. Commun.,* 2014, **50**, 219-221.
13. Y. Nishibayashi, I. Wakiji, M. Hidai, *J. Am. Chem. Soc.,* 2000, **122**, 11019-11020.
14. M. Yoshida, T. Gotou, M. Ihara, *Chem. Commun.,* 2004, **9**, 1124-1125.
15. D. G. Y u, X. Wang, R. Y. Zhu, S. Luo, X. B. Zhang, B. Q. Wang, Z. J. Shi, *J. Am. Chem. Soc.,* 2012, **134**, 14638-14641.
16. Z. C. Cao, D. G. Yu, R. Y. Zhu, J. B. Wei, Z. J. Shi, *Chem. Commun.,* 2015, **51**, 2683-2686.
17. S. Akkarasamiyo, J. Margalef, J. S. M. Samec, *Org. Lett.,* 2019, **21**, 4782-4787.
18. U. Díaz, D. Brunel, A. Corma, *Chem. Soc. Rev.,* 2013, **42**, 4083-4097.
19. C. Yu, J. He, *Chem. Commun.,* 2012, **48**, 4933-4940.
20. W. H. Peng, Y. Y. Lee, C. N. Wu, K. C. W. Wu, *J. Mater. Chem.,* 2012, **43**, 23181-85.
21. B. Liu, H. Liu, C. Wang, L. Liu, S. Wu, J. Guan, Q. Kan, *Appl. Catal., A,* 2012, **443–444**, 1-7.
22. N. R. Shiju, A. H. Alberts, S. Khalid, D. R. Brown, G. Rothenberg, *Angew. Chem., Int. Ed.,* 2011, **50**, 9615 - 9619.
23. L. Xu, C. H. Wang, J. Q. Guan, *J. Solid State Chem.,* 2014, **213**, 250-255.
24. N. A. Brunelli, S. A. Didas, K. Venkatasubbaiah, C. W. Jones, *J. Am. Chem. Soc.,* 2012, **134**, 13950-13953.
25. N. Aider, A. Smuszkiewicz, E. Pérez-Mayoral, E. Soriano, R. M. Martín-Aranda, D. Halliche, S. Menad, *Catalysis Today*, 2014, **227**, 215-222.
26. S. Das, A. Goswami, N. Murali, T. Asefa, *ChemCatChem*, 2013, ***5***, 910-919.
27. H. Wang, L. Z. Liang, W. J. Zhang, J. Y. Han, *J. Porous Mater.*, 2012, **19**, 889-895.
28. P. Kasinathan, C. Lang, J. Schnee, C. D'Haese, E. M. Gaigneaux, A. Jonas, A. Fernandes, *Chemistry - A European Journal,* 2019, **25**, 1–11.
29. R. Ryoo, M. J. Kim, *Chem. Commun.,* 1997, (***22***), 2225-2226.
30. D. Zhao, J. Feng, Q. Huo, N. Melosh, G. H. Fredrickson, B. F. Chmelka, G. D. Stucky, *Science,* 1998, **279**, 548-552.
31. M. V. Landau, E. Dafa, M. L. Kaliya, T. Sen, M. Herskowitz, Microporous and mesoporous materials, 2001, **49**, 65-81.
32. H. Hamdan, S. Endud, H. He, M. N. M. Muhid, J. Klinowski, *J. Chem. Society, Faraday Transactions,* 1996, **92**, 2311-2315.
33. M. Krishnamurthy, M. S. M. Kamil, C. K. Krishnan, *Microporous and Mesoporous Materials*, 2016, **221**, 23-31.
34. R. Vidruk, M.V. Landau, M. Herskowitz, V. Ezersky, A. Goldbourt, *J. Catal.,* 2011, **282**, 215-227
35. F. R. Chen, J. G. Davis, J. J. Fripiat, *J. Catal.,* 1992, **133**, 263-278.
36. M. A. Ardagh, Z. Bo, S. L. Nauert, J. M. Notestein, *ACS Catal.,* 2016, ***6***, 6156-6164.
37. G. Cre´peau, V. Montouillout, A. Vimont, L. Mariey, T. Cseri, F. Mauge, *Journal of Physical Chemistry B,* 2006, **110**, 15172-15185.
38. K. Larmier, C. Chizallet, S. Maury, N. Cadran, J. Abboud, A.-F. Lamic-Humblot, E. Marceau, H. Lauron-Pernot, *Angew. Chem.* 2017, **129**, 236-240.
39. C. M. Parlett, L. J. Durndell, A. Machado, G. Cibin, D. W. Bruce, N. S. Hondow, K. Wilson, A. F. Lee, *Catal. Today,* 2014, **229**, 4 6-55.
40. W. E. Farneth, R. J. Gorte, *Chem. Rev.,* 1995, **95**, 615-635.
41. E. G. Derouane, J. C. Vedrine, R. R. Pinto, P. M. Borges, L. Costa, M. A. N. D. A. Lemos, F. Lemos, F. R. Ribeiro, *Catal. Rev.,* Sci. Eng. 2013, **55**, 454–515.
42. T. Barzetti, E. Selli, D. Moscotti, L. Forni, *J. Chem. Soc., Faraday Trans.* 1996, **92**, 1401–1407.
43. MI. Zaki, MA. Hasan, FA. Al-Sagheer, L. Pasupulety., *Colloids and Surfaces A: Physicochemical and Engineering Aspects 2001,* **190**, 261–274.
44. A. Travert, A. Vimont, A. Sahibed-Dine, M. Daturi, J. C. Lavalley, *Applied Catalysis A: General* 2006, **307** 98–107.
45. E. J. M. Hensen, D. G. Poduval, V. Degirmenci, D. A. J. M. Ligthart, W. Chen, F. Maugé, M. S. Rigutto, J. A. R. V. Veen, *The Journal of Physical Chemistry C*, 2012, **116**, 21416-21429.
46. M. Tamura, K. I. Shimizu, A. Satsuma, *Applied Catalysis A: General,* 2012, **433–434** 135–145.
47. I. S. Pieta, M. Ishaq, R. P. K. Wells, J. A. Anderson, *Applied Catalysis A: General*, 2010, **390**, 127-134.
48. B. M. Reddy, K. N. Rao, G. K. Reddy, A. Khan, S.-E. Park, *The Journal of Physical Chemistry C,* 2007, **111**, 18751-18758.
49. T. Seki, M. Onaka, *J. Mol. Catal., A: Chemical,* 2007, **263**, 115-120.
50. P. A. Cox, M. Reid, A. G. Leach, A. D. Campbell, E. J. King, G. C. Lloyd-Jones, *J. Am. Chem. Soc.,* 2017, **139**, 13156-13165.